Supplement for:

The mixing state of carbonaceous aerosol particles in northern and southern California measured during CARES and CalNex 2010

John F. Cahill[1], Kaitlyn Suski[1], John H. Seinfeld[2], Rahul A. Zaveri[3], Kimberly A. Prather[1,4].

[1]*Dept. of Chemistry and Biochemistry, University of California San Diego, CA*

[2]*Division of Chemistry and Chemical Engineering, California Institute of Technology, Pasadena, CA*

[3]*Atmpspheric Sciences & Global Division, Pacific Northwest National Laboratory, Richland, WA*

[4]*Scripps Institute of Oceanography, University of California San Diego, La Jolla, CA*

**Corresponding author:* kprather@ucsd.edu, 858-822-5312. Fax: 858-534-7042

A-ATOFMS particle transmission and data processing

As stated in the main text the A-ATOFMS can measure sizes between ~100 – 1000 nm. However, due to the transmission efficiency of the aerodynamic lens peaks most particles measured were between 200 – 700 nm, with a mode at ~330nm. The Twin Otter aircraft (CalNex) inlet transmitted ~100% of particles up to 3500 nm (Hegg et al., 2005), and the Gulfstream-1 (CARES) transmitted near unity up to 5000 nm (Zaveri et al., 2012). The Twin Otter inlet is sub-isokinetic while the Gulfstream-1 inlet is isokinetic (leading to the lower size cutoff compared to the Gulfstream-1). However, the transmission of both inlets is near unity within the A-ATOFMS size range (100-1000nm). In both aircraft sampling lines were reasonably similar, ~2 m long and unheated, so no further corrections are warranted. High sensitivity of the A-ATOFMS detectors occasionally led to the acquisition of gas phase species ionized by a laser pulse. These signals were occasionally counted as particles, and were removed from analysis by retroactively raising the peak area threshold above the gas phase baseline. During CalNex sampling inlet pressures were changed after 10 May 2010. However, there was no significant change in size distributions or particle count with the differing inlet pressure..

Extended particle classifications

Particle classifications were established based upon characteristic peaks identified in previous lab studies. The dominant carbonaceous particle types are explained in the main text. Vanadium mixed with OC (V-OC), high mass OC (HMOC), amine (AM), biological (BIO), dust (D), and sea salt (SS) represented 2.78, 0.86, 0.56, 0.30, 0.50, 2.80% of total aerosol measured by the A-ATOFMS, respectively. Vanadium mixed with OC (V-OC) emitted from the combustion of ship fuels composed ~3% of particles measured by the A-ATOFMS (Ault et al., 2009). This particle type has intense peaks at $^{51}V^+$ and $^{67}VO^+$ as well as OC peaks at *m/z* $^{27}C_2H_3^+/CHN^+$, $^{29}C_2H_5^+$, $^{37}C_3H^+$, $^{39}C_3H_3^+/K^+$, and $^{43}C_2H_3O^+/CHNO^+$ (Ault et al., 2009). HMOC consists of OC peaks at *m/z* $^{27}C_2H_3^+/CHN^+$, $^{37}C_3H^+$, $^{39}C_3H_3^+/K^+$ as well as many intense peaks >100 *m/z*. These types likely represent polycyclic aromatic hydrocarbons or other oligomers formed through cooking processes (Silva and Prather, 2000). Occasionally this particle type contained peaks similar to OS that may lead to an overestimation of OS number fractions, especially during CalNex where HMOC was more prevalent (1.42% compared to 0.16% for CalNex and CARES, respectively). However the number fractions of HMOC are significantly smaller than the observed number fraction of OS (28 and 35% for CalNex and CARES, respectively); hence overestimation of OS number fractions is likely small. Amines are OC particles that contain an intense peak at *m/z* $^{56}C_2HNO^+$, $^{59}C_3H_9N^+$,$^{86}(C_2H_5)_2NCH_2^+$, and/or $^{118}(C_2H_5)_3NOH^+$ and originate from agricultural processes, animal husbandry, or photochemical processing (Angelino et al., 2001;Pratt and Prather, 2010;Sorooshian et al., 2008). Biological particles contain an intense $^{40}Ca^+$, $^{56}CaO^+$, and $^{96}Ca_2O^+$ with OC ($^{27}C_2H_3^+/CHN^+$, $^{37}C_3H^+$, $^{39}C_3H_3^+/K^+$), soot ($^{12}C^+$, $^{24}C_2^+$, $^{48}C_3^+$), and phosphate ($^{79}PO_3^-$) peaks (Fergenson et al., 2004;Pratt and Prather, 2010;Russell, 2009). Dusts contained a wide variety of metals (Na, K, Ti, Ca, and Fe), as well as phosphate ($^{79}PO_3^-$) and silicate ($^{44}SiO^-$, $^{60}SiO_2^-$, and $^{103}Si_2O_3^-$). See salt is characterized by an intense sodium peak ($^{23}Na^+$) and chlorine peaks ($^{35}Cl^-$ and $^{37}Cl^-$) as well as clusters of the two ($^{81}Na_2Cl^+$) (Gard et al., 1998;Pratt and Prather, 2010;Silva and Prather, 2000). Typically both dust and sea salt particles are large (SI Figure 1), hence the low number fractions of SS and D particles can mostly be attributed low transmission of the A-ATOFMS for particles of these sizes. Often SS was aged significantly, containing significant nitrate, sulfate, and OC peaks.

Size Dependent Chemistry

SI Figure 1 shows size resolved mixing state for southern (a) and northern (b) California. For both regions the size dependent chemistry was remarkably uniform across the entire measured size range of the A-ATOFMS, with a few exceptions. In both regions most carbonaceous particle types with the lone exception of HP particles (i.e. OC, BB, HP, Aged Soot and Soot) have increased fractions at lower sizes (< 250 nm), though the confidence in these fractions is weak due to low particle counts within this size range. Of all the particle types SS is the only type to have a significant dependence on size, with its fraction greatly increasing as size increases; consistent with typical supermicron size of SS particles. This likely contributed to the increased prevalence of nitrate on these particles discussed in section 3.3 of the main text.

Temporal changes within CARES

A distinct change in chemistry, particle concentrations, and meteorological variables was seen during the CARES study; hence the study was split into two periods, 2 June 2010 – 19 June 2010 (NoCal-1) and 21 June 2010 – 28 June 2010 (NoCal-2) as can be seen in SI Table 1 and SI Figure 2. An increase in A-ATOFMS Soot-OC and BB fractions was seen during NoCal-2, which coincided with a general increase in temperature and particulate matter > 2.5 µm in the region (SI Figure 2). More detail on the differences in chemistry can be found in the main text. It is hypothesized that higher SO_2 and NO_x concentrations during NoCal-2 lead to the growth of soot. Unlike OC:soot ion ratio distributions (Figure 9), sulfate:nitrate ion ratio distributions remained relatively unchanged between NoCal-1 and NoCal-2 (SI Figure 3); hence sulfate was still the most common secondary species present on particles in northern California.

The absence of negative ion spectra

Negative ion spectra were absent in 13% of particles in California. This has previously been attributed to significant amounts of water present on the particle which inhibits the formation of negative ions (Neubauer et al., 1998, 1997). However, due to the low average relative humidity (RH) during the studies, 49±30% and 39±14%, for CalNex and CARES respectively, and typical deliquescent RH thresholds of >60% (Neubauer et al., 1998), it is unlikely that there was significant water present on the particles to justify the lack of negative spectra. Similar conclusions were deduced from modeling of the CARES study (Fast et al., 2012). Further, spectra with only positive ions were less frequent during CalNex (4%) than CARES (24%) despite the higher RH during CalNex. Temporal comparisons of positive only spectra with RH do not indicate any correlation between the two. Further, significantly higher fractions of particles contain negative ion spectra during NoCal-1, 94%, compared to NoCal-2, 62%. This is despite the higher RH of 41±15% compared to 36±12% for NoCal-1 and NoCal-2, respectively. It is hypothesized that for these studies the acquisition of negative ion spectra was dependent on the presence of secondary species, like sulfate or nitrate, rather than the amount of water present.

References

Angelino, S., Suess, D. T., and Prather, K. A.: Formation of aerosol particles from reactions of secondary and tertiary alkylamines: Characterization by aerosol time-of-flight mass spectrometry, Environ Sci Technol, 35, 3130-3138, 2001.

Ault, A. P., Moore, M. J., Furutani, H., and Prather, K. A.: Impact of Emissions from the Los Angeles Port Region on San Diego Air Quality during Regional Transport Events, Environ Sci Technol, 43, 3500-3506, 10.1021/es8018918, 2009.

Fast, J. D., Gustafson, W. I., Berg, L. K., Shaw, W. J., Pekour, M., Shrivastava, M., Barnard, J. C., Ferrare, R. A., Hostetler, C. A., Hair, J. A., Erickson, M., Jobson, B. T., Flowers, B., Dubey, M. K., Springston, S., Pierce, R. B., Dolislager, L., Pederson, J., and Zaveri, R. A.: Transport and mixing patterns over Central California during the carbonaceous aerosol and radiative effects study (CARES), Atmospheric Chemistry and Physics, 12, 1759-1783, DOI 10.5194/acp-12-1759-2012, 2012.

Fergenson, D. P., Pitesky, M. E., Tobias, H. J., Steele, P. T., Czerwieniec, G. A., Russell, S. C., Lebrilla, C. B., Horn, J. M., Coffee, K. R., Srivastava, A., Pillai, S. P., Shih, M. T. P., Hall, H. L., Ramponi, A. J., Chang, J. T., Langlois, R. G., Estacio, P. L., Hadley, R. T., Frank, M., and Gard, E. E.: Reagentless detection and classification of individual bioaerosol particles in seconds, Anal Chem, 76, 373-378, Doi 10.1021/Ac034467e, 2004.

Gard, E. E., Kleeman, M. J., Gross, D. S., Hughes, L. S., Allen, J. O., Morrical, B. D., Fergenson, D. P., Dienes, T., Galli, M. E., Johnson, R. J., Cass, G. R., and Prather, K. A.: Direct observation of heterogeneous chemistry in the atmosphere, Science, 279, 1184-1187, 1998.

Hegg, D. A., Covert, D. S., Jonsson, H., and Covert, P. A.: Determination of the transmission efficiency of an aircraft aerosol inlet, Aerosol Science and Technology, 39, 966-971, Doi 10.1080/02786820500377814, 2005.

Neubauer, K. R., Johnston, M. V., and Wexler, A. S.: On-line analysis of aqueous aerosols by laser desorption ionization, International Journal of Mass Spectrometry and Ion Processes, 163, 29-37, 1997.

Neubauer, K. R., Johnston, M. V., and Wexler, A. S.: Humidity effects on the mass spectra of single aerosol particles, Atmospheric Environment, 32, 2521-2529, 1998.

Pratt, K. A., and Prather, K. A.: Aircraft measurements of vertical profiles of aerosol mixing states, Journal of Geophysical Research, 115, 10.1029/2009jd013150, 2010.

Russell, S. C.: Microorganism characterization by single particle mass spectrometry, Mass spectrometry reviews, 28, 376-387, 10.1002/mas.20198, 2009.

Silva, P. J., and Prather, K. A.: Interpretation of Mass Spectra from Organic Compounds in Aerosol Time-of-Flight Mass Spectrometry, Anal Chem, 72, 3553-3562, 10.1021/ac9910132, 2000.

Sorooshian, A., Murphy, S. N., Hersey, S., Gates, H., Padro, L. T., Nenes, A., Brechtel, F. J., Jonsson, H., Flagan, R. C., and Seinfeld, J. H.: Comprehensive airborne characterization of aerosol from a major bovine source, Atmospheric Chemistry and Physics, 8, 5489-5520, 2008.

Zaveri, R. A., Shaw, W. J., Cziczo, D. J., Schmid, B., Ferrare, R. A., Alexander, M. L., Alexandrov, M., Alvarez, R. J., Arnott, W. P., Atkinson, D. B., Baidar, S., Banta, R. M., Barnard, J. C., Beranek, J., Berg, L. K., Brechtel, F., Brewer, W. A., Cahill, J. F., Cairns, B., Cappa, C. D., Chand, D., China, S., Comstock, J. M., Dubey, M. K., Easter, R. C., Erickson, M. H., Fast, J. D., Floerchinger, C., Flowers, B. A., Fortner, E., Gaffney, J. S., Gilles, M. K., Gorkowski, K., Gustafson, W. I., Gyawali, M., Hair, J., Hardesty, R. M., Harworth, J. W., Herndon, S., Hiranuma, N., Hostetler, C., Hubbe, J. M., Jayne, J. T., Jeong, H., Jobson, B. T., Kassianov, E. I., Kleinman, L. I., Kluzek, C., Knighton, B., Kolesar, K. R., Kuang, C., KubC!tovC, A., Langford, A. O., Laskin, A., Laulainen, N., Marchbanks, R. D., Mazzoleni, C., Mei, F., Moffet, R. C., Nelson, D., Obland, M. D., Oetjen, H., Onasch, T. B., Ortega, I., Ottaviani, M., Pekour, M., Prather, K. A., Radney, J. G., Rogers, R. R., Sandberg, S. P., Sedlacek, A., Senff, C. J., Senum, G., Setyan, A., Shilling, J. E., Shrivastava, M., Song, C., Springston, S. R., Subramanian, R., Suski, K., Tomlinson, J., Volkamer, R., Wallace, H. W., Wang, J., Weickmann, A. M., Worsnop, D. R., Yu, X. Y., Zelenyuk, A., and Zhang, Q.: Overview of the 2010 Carbonaceous Aerosols and Radiative Effects Study (CARES), Atmos. Chem. Phys., 12, 7647-7687, 10.5194/acp-12-7647-2012, 2012.

Campaign	Flight Name[1] (yyyymmdd)	Temperature (°C)	RH (%)	UF-CPC (#/ccm)*10^4	CPC (#/ccm)*10^3	PCASP/UHSAS[2] (#/ccm)*10^3
Calnex	20100504a	20.8 ± 2.6	39 ± 12	1.5 ± 1.0	11.6 ± 5.0	1.5 ± 0.4
	20100505a	18.8 ± 2.4	51 ± 33	1.0 ± 0.5	N/A	5.8 ± 5.1
	20100506a	17.0 ± 1.9	58 ± 54	1.2 ± 0.6	10.6 ± 4.5	1.4 ± 0.4
	20100507a	21.6 ± 2.3	35 ± 22	1.4 ± 0.6	11.4 ± 4.3	3.3 ± 3.9
	20100510a	13.7 ± 1.3	61 ± 37	1.3 ± 0.7	11.0 ± 4.9	0.7 ± 0.3
	20100512a	18.8 ± 3.2	35 ± 15	1.4 ± 0.8	11.2 ± 5.3	2.9 ± 3.8
	20100513a	21.3 ± 3.9	31 ± 14	1.1 ± 0.7	8.2 ± 4.1	1.0 ± 0.6
	20100514a	16.6 ± 2.3	64 ± 10	1.5 ± 0.8	12.1 ± 5.2	1.3 ± 0.4
	20100515a	19.3 ± 3.2	56 ± 29	1.2 ± 0.5	10.8 ± 4.0	1.6 ± 0.4
	All Flights	18.6 ± 3.6	48 ± 31	1.3 ± 0.7	10.9 ± 4.8	2.2 ± 2.9
CARES	20100603a	20.2 ± 4.0	60 ± 7	2.2 ± 1.9	18.1 ± 12.5	N/A
	20100606a	23.5 ± 2.1	55 ± 5	2.2 ± 1.8	18.0 ± 11.4	N/A
	20100606b	24.4 ± 6.7	41 ± 9	1.3 ± 1.0	10.8 ± 6.4	N/A
	20100608a	20.1 ± 2.0	56 ± 10	2.0 ± 2.0	1.0 ± 0.8	N/A
	20100608b	20.5 ± 4.6	40 ± 14	1.3 ± 1.3	0.9 ± 0.7	N/A
	20100610a	17.4 ± 3.8	38 ± 8	1.7 ± 1.0	1.0 ± 0.3	1.1 ± 0.6
	20100612a	20.9 ± 2.7	28 ± 2	1.2 ± 1.8	0.5 ± 0.7	0.9 ± 0.2
	20100612b	25.1 ± 2.5	25 ± 4	1.4 ± 1.0	0.7 ± 0.3	1.5 ± 0.8
	20100614a	23.8 ± 2.9	32 ± 9	2.8 ± 2.4	1.3 ± 1.0	2.1 ± 1.9
	20100615a	17.3 ± 1.9	55 ± 12	2.2 ± 1.9	1.1 ± 1.5	1.6 ± 1.9
	20100615b	20.7 ± 5.5	42 ± 9	1.5 ± 0.9	1.1 ± 0.6	2.6 ± 0.8
	20100618a	21.5 ± 5.7	25 ± 12	2.2 ± 1.6	1.1 ± 0.8	2.3 ± 1.9
	20100619a	18.5 ± 3.6	39 ± 9	2.0 ± 1.0	1.5 ± 0.7	1.9 ± 1.0
	20100621a	18.8 ± 1.7	43 ± 7	1.9 ± 2.2	1.1 ± 1.2	1.9 ± 1.1
	20100621b	25.2 ± 6.6	21 ± 7	1.1 ± 0.9	0.8 ± 0.5	1.8 ± 1.1
	20100623a	19.6 ± 4.0	40 ± 10	0.8 ± 1.2	0.6 ± 1.0	3.2 ± 1.0
	20100623b	25.0 ± 6.8	30 ± 8	1.3 ± 0.7	0.9 ± 0.5	3.9 ± 1.8
	20100624a	19.1 ± 2.1	44 ± 15	2.1 ± 2.1	1.0 ± 1.0	1.2 ± 0.8
	20100624b	22.1 ± 3.8	37 ± 8	2.1 ± 1.6	2.4 ± 3.1	2.3 ± 1.0
	20100627a	25.6 ± 2.1	41 ± 10	0.6 ± 0.9	0.5 ± 0.6	3.4 ± 3.1
	20100628a	28.2 ± 2.6	38 ± 7	1.0 ± 1.0	0.8 ± 0.8	3.9 ± 1.9
	20100628b	35.5 ± 5.7	25 ± 4	0.8 ± 0.5	0.6 ± 0.3	3.5 ± 1.6
	All Flights	22.4 ± 5.7	39 ± 14	1.6 ± 1.6	2.7 ± 6.1	2.2 ± 1.7
	NoCal-1	21.0 ± 4.7	41 ± 14	1.9 ± 1.6	3.9 ± 7.6	1.8 ± 1.4
	NoCal-2	24.3 ± 6.5	36 ± 1	1.3 ± 1.5	1.0 ± 1.3	2.7 ± 1.9

[1] Flight names labeled "a" occurred in the morning, while those labeled with a "b" were in the afternoon

[2] PCASP was used during CalNex while the UHSAS was used during CARES

SI Table 1: Mean (± std dev) meteorological data and particle concentrations over all of CalNex, CARES, NoCal-1, and NoCal-2.

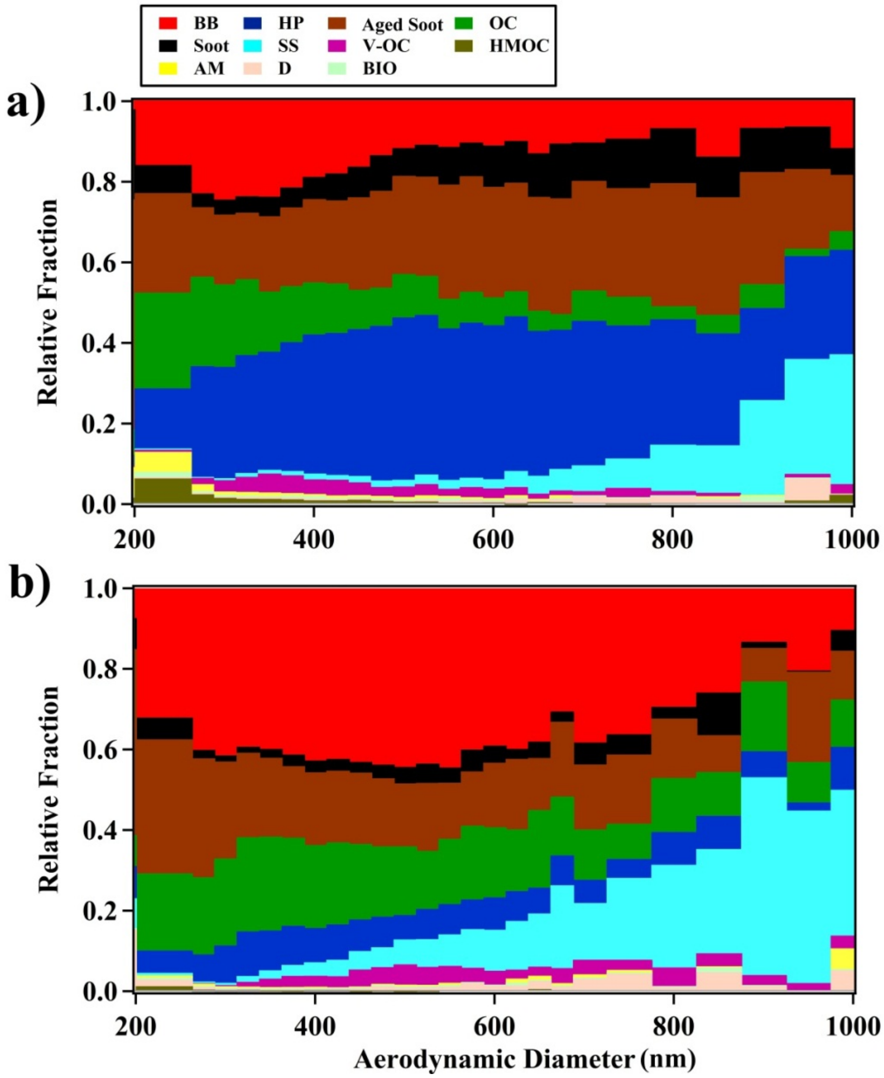

SI Figure 1: Size resolved mixing state for (a) southern and (b) northern California.

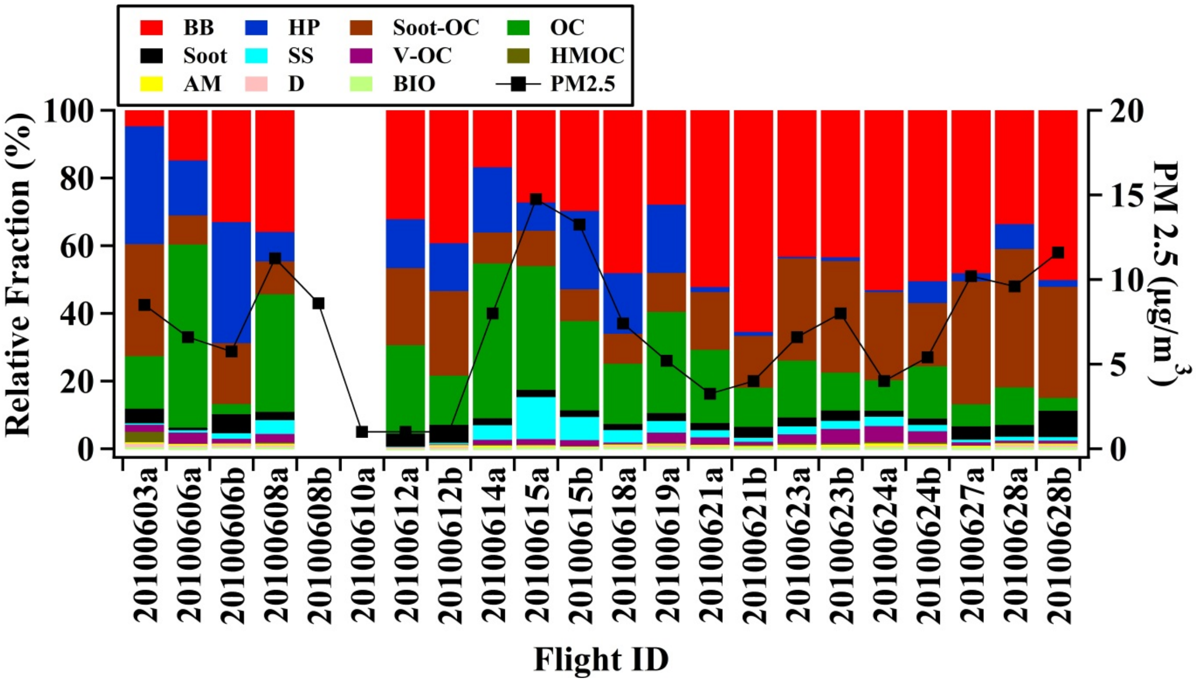

SI Figure 2: A-ATOFMS relative fractions of particle types and average PM2.5 mass concentrations for each flight during the CARES study. Flight labels indicate the date of the flight and if it was in the morning (a) or afternoon (b). A change in chemistry and a general increase in PM2.5 mass were observed after 6/19/10.

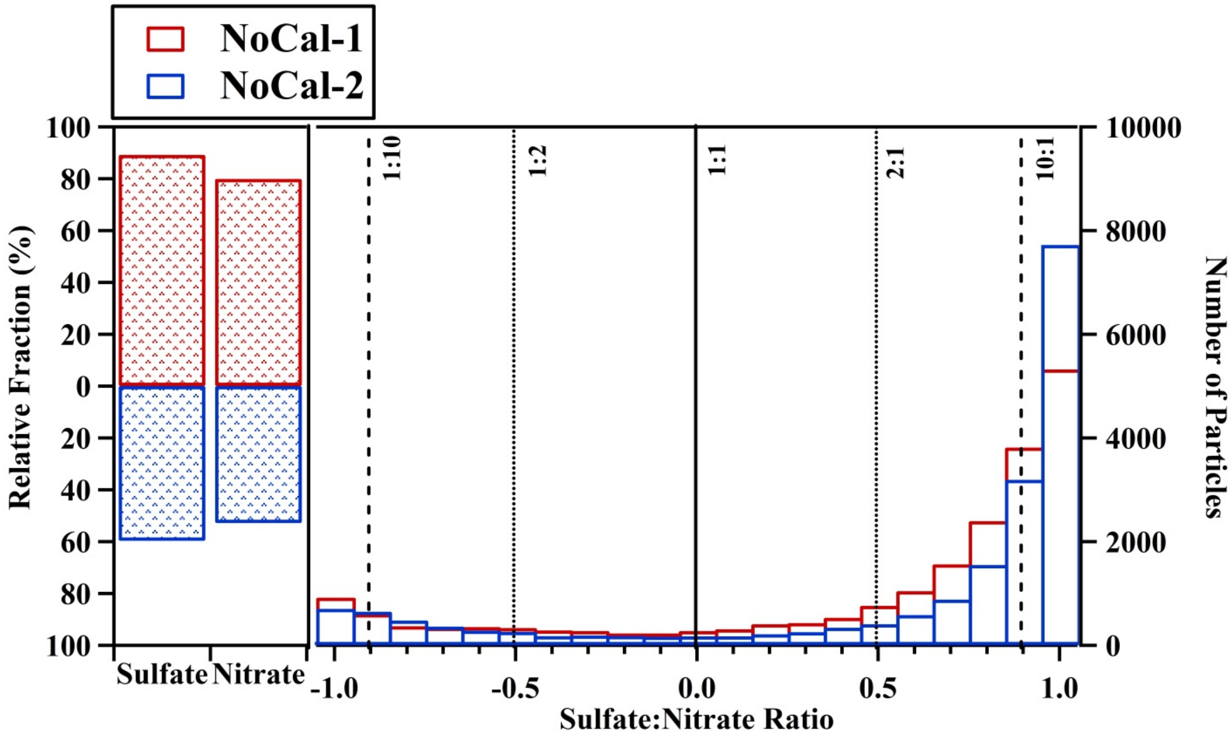

SI Figure 3: Fraction of particles containing sulfate and nitrate with RPA > 0.5% in NoCal-1 (red) and NoCal-2 (blue, left panel). Sulfate:nitrate peak ion ratio distributions are shown in (right panel). Values < 0 indicate more soot than nitrate and values > 0 indicate more sulfate than soot. Ratios representing 1:1, 2:1, and 10:1 are shown by solid, dotted, and dashed lines respectively.